MOLECULAR AND CELLULAR BIOLOGY, Sept. 1987, p. 3057–3064
0270-7306/87/093057-08$02.00/0

Vol. 7, No. 9

Mouse Nerve Growth Factor Gene: Structure and Expression

MARK J. SELBY,[1] ROBERT EDWARDS,[1,2] FRANK SHARP,[2] AND WILLIAM J. RUTTER[1]*

Hormone Research Institute and Department of Biochemistry and Biophysics,[1] and Department of Neurology,[2] University of California, San Francisco, California 94143

Received 19 March 1987/Accepted 22 June 1987

The organization and biologically significant sequences of the entire mouse nerve growth factor (NGF) gene have been determined. The gene spans 45 kilobases and contains several small 5′ exons. Transcription of the gene results in four different mRNA species, which can be accounted for by alternative splicing and independent initiation from two promoters. These transcripts encode proteins which have divergent N termini and the NGF moiety at their C termini. The levels of the various NGF transcripts have been determined in different tissues and throughout postnatal development. We have also examined the expression of these transcripts in the brain in response to specific early sensory deprivation. The results suggest that the expression of NGF mRNA during postnatal development is regulated independently of the formation of complex neural networks.

Developing sympathetic and sensory neurons require nerve growth factor (NGF) (17, 28) for survival. Of these cells, a significant proportion dies in the first few weeks after birth (approximately 30% for the sympathetic neurons in the rat superior cervical ganglion). Injection of antibodies to NGF during the development of sympathetic and sensory neurons results in the death of these cells (9, 18). Administration of purified NGF permits the survival of all these cells, including those that would normally die (1). NGF thus appears to be a modulator of normal, programmed cell death. During development, neurons which obtain NGF survive, while those that do not, die.

Sympathetic and sensory neurons acquire NGF via a specific, retrograde axonal transport system (27). Transecting the axons of developing sympathetic neurons in the superior cervical ganglion causes the cells with lesions to die. Similarly, death occurs after administration of antibodies to NGF. Systemic injection of NGF permits survival of the axotomized cells, presumably by providing NGF directly to the cell body (11). Cells responding to NGF have NGF receptors on their processes and on their cell bodies (12, 14). The presence of a retrograde axonal transport system for NGF suggests that neurons obtain NGF from the cells that they innervate. The fact that NGF protein and mRNA levels correlate with the density of innervation in peripheral organs supports this idea (15, 25). The development of normal adult neural networks thus appears to depend on NGF gene expression in cells interacting with the dependent neurons.

An NGF cDNA derived from the mouse submaxillary gland has been isolated and characterized (24). It predicts a precursor protein with the NGF moiety at the C terminus. We have also described a cDNA representing a shorter NGF transcript that predominates in all tissues other than the mouse submaxillary gland and the placenta from several species (8). The virtual identity of the nucleotide sequence of the two cDNAs suggests that they were derived from the same gene. A portion of the human gene corresponding to the mouse cDNA but lacking the 5′ sequence has been reported (6, 29).

We present here the structure of the entire mouse NGF gene, as well as the sequences of two additional cDNAs, and we show that the four cDNAs result from alternative splicing and the use of independent promoter elements. We also report the distribution of the NGF mRNAs in different tissues and throughout postnatal development. In sensory deprivation experiments, the level of steady-state NGF transcripts appears to be independent of the formation of certain neural connections.

MATERIALS AND METHODS

Isolation and characterization of cDNA clones. To conserve the full 5′ ends of the mRNA, we constructed a λgt10 submaxillary gland cDNA library by using random primers for synthesis of the first strand and a modification of the Gubler-Hoffman method for synthesis of the second strand (8, 10). We screened the library with oligonucleotides as previously described (8) and sequenced the unique clones of interest (identified by comparing dideoxy T tracks) on both strands (20, 23).

RNA analysis. Freshly dissected tissue from several animals in different litters was pooled and homogenized with a polytron in guanidinium isothiocyanate (4). Total RNA was prepared by LiCl precipitation (3) or by CsCl density gradient sedimentation, followed by phenol-chloroform extraction and two ethanol precipitations. RNA content was determined spectrophotometrically at 260 nm after the second precipitation.

Primer extension assays were performed with a uniformly labeled single-stranded 129-base primer as previously described (8).

Uniformly labeled S1 nuclease probes were made from M13 subclones of the cDNAs obtained from the above submaxillary gland library with the same 22-base primer (complementary to +328 to +306) and two of four labeled nucleotides (8). The extended primer was cleaved in the M13 polylinker and isolated after electrophoresis on a 5% polyacrylamide–urea gel. The resulting single-stranded probe (50,000 cpm) was coprecipitated with 10 to 25 μg of a total RNA sample, heated to 85°C in 80% formamide for 15 min, and hybridized overnight at 45°C. S1 nuclease digestion with 100 U of enzyme (P-L Biochemicals) at 37°C for 90 min was followed by extraction, ethanol precipitation, and electrophoresis on a 5% acrylamide–urea gel. Laser densitometry was used to quantitate the relative amounts of NGF mRNA hybridizing specifically to a given probe and to

* Corresponding author.

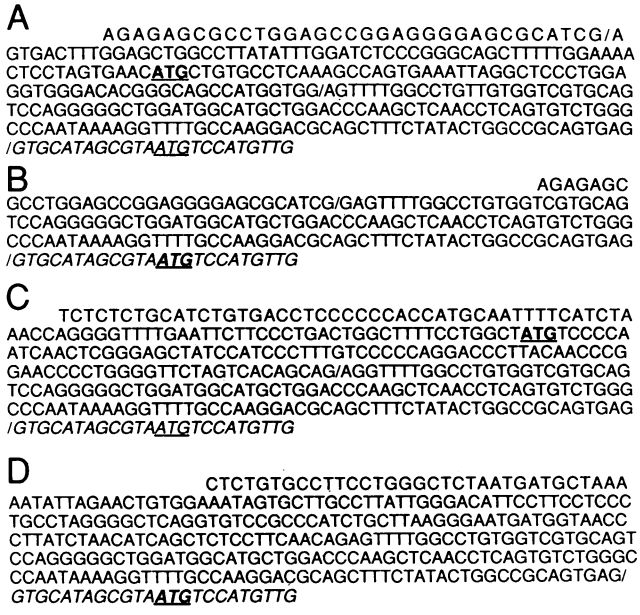

FIG. 1. Nucleotide sequence of NGF cDNAs A through D. Slashes denote the presence of intervening sequences in the cDNAs. In-frame AUG codons have been underlined. The presumptive initiation methionine codons are in bold letters.

quantitate ethidium bromide-stained nondenaturing agarose gels of the RNA samples, which were then used to normalize the S1 nuclease results to total RNA (mostly rRNA).

Isolation and characterization of genomic bacteriophage clones. A mouse phage library (*Mbo*I partial digests of BALB/c embryonic DNA ligated into Bam-Charon 28, Leder no. 10277) was screened with nick-translated probes (19) representing various portions of the NGF cDNA and genomic subclones. Hybridizing phage were purified, restriction mapped, and subcloned into M13 vectors for sequencing. All exons and their immediate flanking DNA were sequenced by the dideoxy method (23). The size of the intron not represented in the phage clones was estimated by hybridization of genomic DNA with probes derived from the 3′ (pH3) and 5′ (pH2) ends of the respective 5′ and 3′ phage.

Lesion experiments. At birth and at 1, 2, and 3 weeks after birth, the right whisker pad was removed from individual mice from several litters, with ice as anesthesia. When the mice were 4 weeks old, they were sacrificed and one of us (F.S.) dissected regions (approximately 3 by 3 mm) encompassing the somatosensory cortex, as well as the dorsolateral brainstem (including the fifth nerve nucleus). RNA preparation and S1 nuclease assay were performed as described above.

RESULTS

Different NGF precursors predicted by cDNA clones. We have previously identified two transcripts that derive from the NGF gene. The first mRNA shown in Fig. 1 is the originally described, long NGF transcript (24), here termed transcript A. A cDNA representing the short transcript (transcript B) was identified as hybridizing to an oligonucleotide complementary to the third exon of A (+205 to +188) and failing to hybridize to an oligonucleotide from the second exon of A (+145 to +124) (8). (Transcript B was previously suspected to exist on the basis of S1 nuclease protection and primer extension experiments.) Of the six independent cDNA clones which showed this hybridization pattern, three represented NGF transcript B, two represented prematurely terminated transcript A (having part but not all of the second exon of A), and one had an entirely different sequence 5′ to the junction between the second and third exons of transcript A. This third distinct cDNA (representing transcript C [Fig. 1]) predicts a novel NGF precursor, with a new exon replacing the first two exons (of transcript A). The protein encoded by the new exon (IA [see Fig. 3]) would replace the 20 N-terminal residues of the original, long NGF precursor protein with a totally different 27 amino acids, resulting in a prohormone that is approximately 700 daltons larger. Because of the apparent abundance of transcript C, we sequenced an additional 20 cDNA clones obtained by the same hybridization protocol. Among them we found an additional unique clone, cDNA D (Fig. 1). Transcript D also diverges 5′ to the border of exons 2 and 3, but does not contain a new in-frame AUG; it thus predicts a precursor identical to that encoded by transcript B. To determine the relative in vivo levels of transcripts C and D, we performed S1 nuclease analysis on submaxillary gland RNA, with uniformly labeled single-stranded probes derived from the respective cDNA clones (Fig. 2). Both transcripts C and D were much less abundant (by 2 to 3 orders of magnitude) than A or B were, although transcript D was present in greater quantities than transcript C was (Fig. 1B).

Structure of the mouse NGF gene. To understand the structural basis for these multiple transcripts, it was necessary to define the organization of the NGF gene and in particular, its 5′ portion. Using NGF cDNA A as a probe, we isolated a phage containing the two 3′ exons (exons III and IV [Fig. 3A]). Exon IV encoded all of mature NGF (118 amino acids), as well as an additional 125 amino acids in the amino-terminal direction. Exon IIIB comprised 124 base pairs (bp) in the non-NGF moiety of the predicted prohormone. Exon IIIA was juxtaposed next to IIIB and accounted for all the unique 5′ DNA sequences of cDNA D. The library was further screened with a fragment from the 5′ end of cDNA A, which yielded a phage containing an additional 127-bp exon (exon II) in the 5′ direction. To obtain the remaining 33 bp of the transcribed portion of the gene, we rescreened the library with a probe specific for this region (5′ end of exon II). Additional clones identified in this way extended 2.5 kilobases (kb) further in the 5′ direction but lacked the final 33 bp of transcripts A and B. Repeated screening of two mouse phage genomic libraries with a unique sequence in the most 5′ region of the above genomic clones failed to yield phage that had the missing exon.

The identification of cDNA C provided a new sequence with which to isolate the 5′ end of the NGF gene. Using the most 5′ *Eco*RI fragment of cDNA C as a probe, we identified genomic clones possessing the exon unique to transcript C (exon IA [Fig. 3A and C]) and in addition, the missing 33-bp exon of transcripts A and B (exon IB [Fig. 3A and C]). Only 142 bp separated these two 5′ exons (Fig. 3C). Although these phage clones contained approximately 12 kb of genomic DNA in the 3′ direction, they did not overlap with the previously isolated 3′ phage clone. Neither probes specific for the 3′ end of the 5′ phage clone (pH2) nor for the 5′ end of the 3′ phage clone (pH3) hybridized to any single restriction fragment on a Southern blot of genomic DNA (Fig. 3B). The largest bands hybridizing to the probes were found in *Eco*RV-digested DNA. The pH3 DNA hybridized to a 7.0-kb fragment extending 3′ from an *Eco*RV restriction site in the intron between exons I and II. PH2 hybridized to an ~23-kb

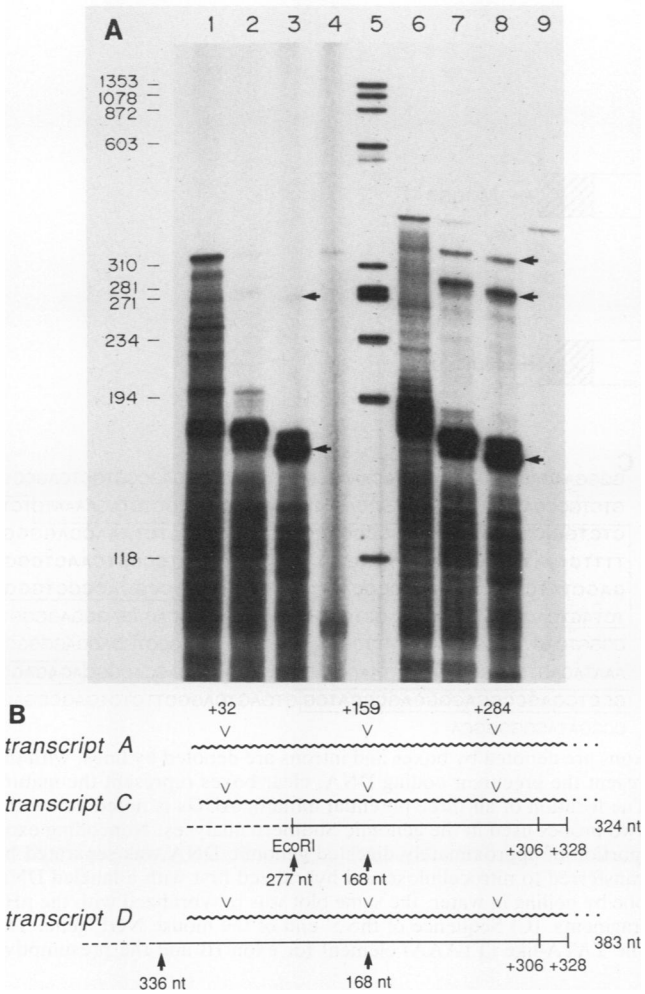

FIG. 2. S1 nuclease analysis of submaxillary gland RNA with cDNA clones C and D as probes. (A) A 20-μg sample of male mouse submaxillary gland RNA (lanes 1 to 3 and 6 to 8) was assayed with single-stranded probes derived from clones C (lanes 1 to 4) and D (lanes 6 to 9). The following amounts of S1 nuclease per reaction were used: 1 U in lanes 1 and 6, 10 U in lanes 2 and 7, and 100 U in lanes 3 and 8; tRNA controls (20 μg in lanes 4 and 9) were digested with 10 U of S1 nuclease. Arrows indicate the protected fragments, with the two major transcripts represented by the lower, intense band. The numbers to the left of the gel indicate the sizes (in bases) of the fragments. (B) Diagram of the S1 nuclease probes derived from cDNAs C and D. An oligonucleotide complementary to +328 to +306 (of transcript A) was annealed to the appropriate M13 subclone, extended with the Klenow fragment of *Escherichia coli* DNA polymerase, digested in the M13 polylinker (represented by the dashed lines), and prepared from a 5% urea–polyacrylamide gel. cDNA C has an internal *Eco*RI site so the relevant (3′) subclone was used to generate the probe. The size of the probes is shown to the right in nucleotides (nt). The arrows below indicate the predicted sites of cleavage by S1 nuclease, along with the sizes of the protected fragments.

fragment extending 5′ from an *Eco*RV site in the intron between exons II and III. This indicates a minimum size of around 32 kb for the intron between exons I and II. Further mapping revealed the sizes of the second and third introns to be approximately 4 and 6 kb, respectively. Thus, the NGF gene comprises more than 43 kb. The sequences of all the exon-intron boundaries followed the consensus signals for RNA splicing (21) (data not shown). Figure 4 shows the various NGF transcripts in relation to the NGF gene. A comparison of the organization of the murine NGF gene with the known portion of the human NGF gene reveals a perfect correspondence in the sizes of the two most 3′ exons and in the location of the introns (6, 29) (Fig. 3A).

Primer extension experiments have already defined the transcription start sites of the two major NGF transcripts (A and B) (24). The sequence upstream contained a TATA-like element, TTAAA, at −28 and an unusually GC-rich (68%) region at −50 to −140 relative to the cap site (Fig. 3C). Because of the extremely low abundance of transcript C, we could not clearly identify the transcriptional start site by primer extension or S1 nuclease analyses (with a shorter genomic probe, rather than the larger, and therefore, more sensitive, cDNA probe used in Fig. 2). The absence of an upstream consensus splice acceptor sequence and the presence of an in-frame upstream termination codon suggest that translation initiates at the AUG indicated in Fig. 1. Examination of the genomic sequence flanking the 5′ end of cDNA C does not reveal a TATA element (5) or sequences similar to the simian virus 40 21-bp repeat that have been observed in several other genes (22, 30). Two CCAAT (2) boxes were observed at positions −79 and −180 (data not shown). To determine whether transcript C is conserved, we probed a Southern blot of human genomic DNA with a 5′ sequence unique to cDNA C and detected a single hybridizing band (data not shown). A probe containing the 5′ end of transcript D (exon IIIA) and extending 200 bp in the 5′ direction was fully protected from S1 nuclease digestion with mouse submaxillary gland RNA (data not shown). This suggests that this cDNA may represent a partially spliced intermediate in the processing of the primary NGF transcript.

Expression of both NGF transcripts A and B in many adult tissues. The distribution of NGF transcripts was determined in adult mouse tissues. Primer extension experiments with a single-stranded primer (complementary to +328 to +199 of transcript A) with a high specific activity showed that in contrast to the salivary gland, where transcript A (the longer extension product) predominates, all the peripheral organs and brain regions tested had transcript B (the short product) as the major NGF mRNA (Fig. 5). Densitometry showed ratios of approximately 3:1 (A:B) for the submaxillary gland and 1:4 for the other tissues. Intermediate extension products presumably result from premature termination; this would produce a modest underestimation in the abundance of transcript A. Further, it is possible that the long extension product represents transcripts C and D (as well as A); cDNAs C and D are virtually the same length (at their 5′ ends) as transcripts A and B. However, as transcripts C and B are very rare even in the submaxillary gland, it is likely that most of the long extension product represents transcript A. There appears to be no sexual dimorphism in the NGF gene expression in the mouse brain (Fig. 5, lanes 5 and 6), as there is in the submaxillary gland.

Parallel increase of NGF transcripts throughout early postnatal development. To determine whether the expression of the various NGF transcripts correlates with a phase of neural development, we have used a sensitive S1 nuclease assay to distinguish the transcripts in RNA samples obtained at different times after birth. The single-stranded, uniformly labeled ([^{32}P]dCTP and [^{32}P]dGTP) probe extends from +328 past the cap site of transcript A (into the M13 polylinker) and hence distinguishes transcript A from other transcripts divergent at the +159 splice junction (mostly transcript B). In the cortex, the level of NGF transcripts increased during the weeks after birth and reached a peak at 20 days; it then

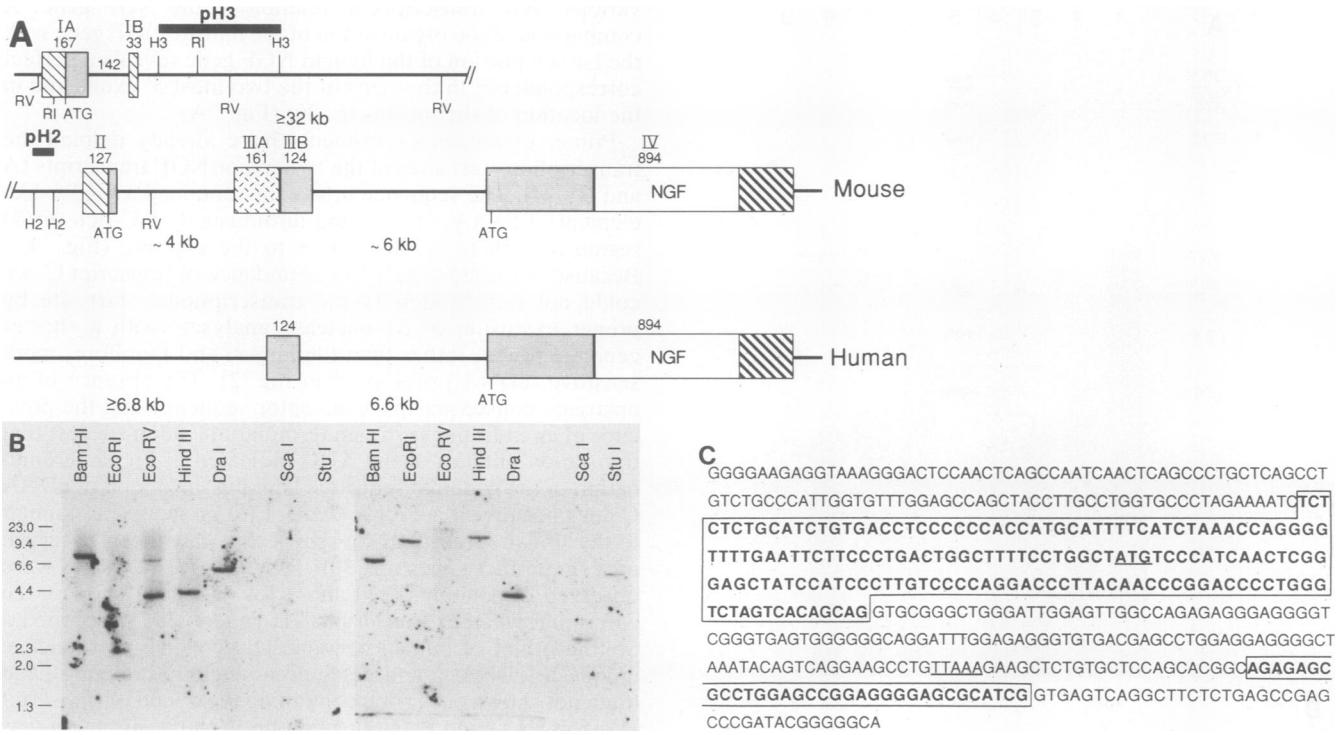

FIG. 3. (A) Organization of the mouse and human NGF genes. The exons are denoted by boxes and introns are denoted by lines, with the sizes and nomenclature for the exons given above. The dark boxes represent the precursor coding DNA, clear boxes represent the mature NGF, and hatched boxes represent the 5′ and 3′ untranslated regions. The location of all three potential initiator AUGs is noted below the corresponding exon. The dark bars above the introns correspond to the two probes used in the genomic Southern analyses. Noncoding exon IIIA is indicated. (B) Southern blot of mouse genomic DNA. A 10-μg portion of approximately digested genomic DNA was separated by electrophoresis in a 0.9% agarose gel. After denaturation, the gel was transferred to nitrocellulose and hybridized first with a labeled DNA fragment from the pH2 genomic subclone (right). After removing this probe by boiling in water, the same blot was rehybridized with the pH3 subclone (left). The numbers to the left indicate the sizes (in bases) of fragments. (C) Sequence of the 5′ end of the mouse NGF gene. The sequences of the two exons, IA and IB, are in bold type and boxed. The TATA-like (TTAAA) element for exon IB and the presumptive initiator methionine in exon IA are both underlined.

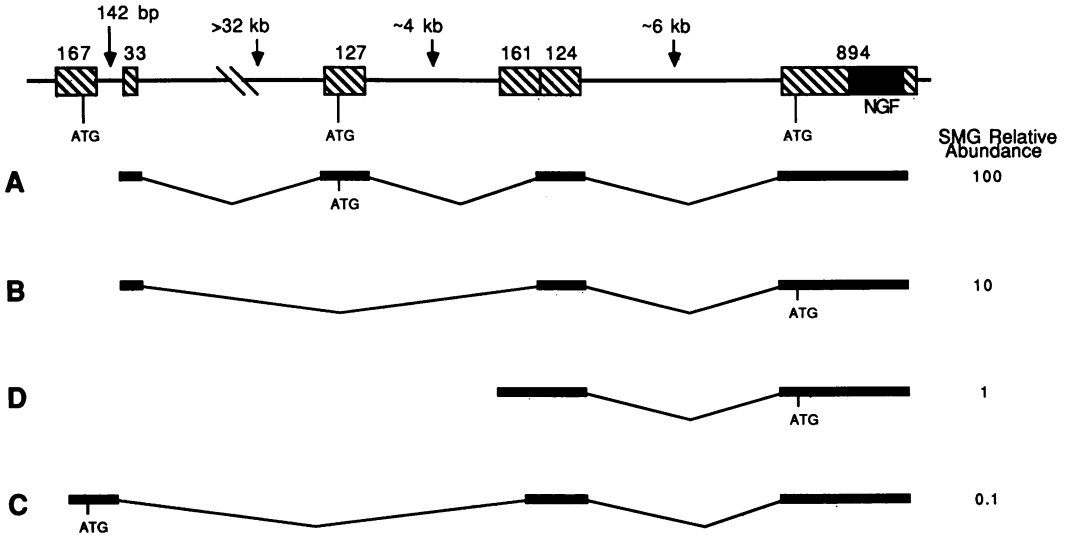

FIG. 4. Diagrammatic representation of the predicted NGF transcripts in relation to the gene. The gene is shown at the top with exons as boxes and introns as lines. The size of the exons (in base pairs) is shown above the boxes; the size of the introns is also shown; mature NGF is stippled. The four identified NGF transcripts are depicted below in order of decreasing submaxillary gland (SMG) abundance (A, B, D, and then C). The thick lines represent sequences formed in the mature RNA, and the thin lines represent regions that are removed by splicing of a primary transcript. The presumed sites for initiation of translation are indicated (ATG).

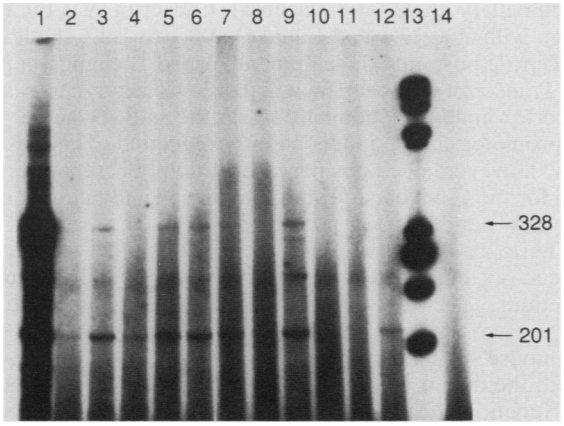

FIG. 5. Primer extension analysis of NGF transcripts from various mouse tissues. A primer extending from +328 to +199 (of transcript A) was uniformly labeled with [^{32}P]dCTP and [^{32}P]dGTP. The primer was extended with reverse transcriptase after annealing to the following amounts of RNA: 10 μg of female submaxillary gland total RNA (lane 1), 3 μg of small intestinal poly(A)$^+$ RNA (lane 2), 5 μg of kidney poly(A)$^+$ RNA (lane 3), 1 μg of heart poly(A)$^+$ RNA (lane 4), 3 μg of male and female brain poly(A)$^+$ RNAs (lanes 5 and 6, respectively), 3 μg of deep gray matter poly(A)$^+$ RNA (lane 9), 1 μg of brainstem poly(A)$^+$ RNA (lane 10), 1 μg of cerebellum poly(A)$^+$ RNA (lane 11), 3 μg of newborn brain poly(A)$^+$ RNA (lane 12), *Hae*III digest of φX174 DNA (lane 13), 20 μg of yeast tRNA (lane 14). Arrows indicate the major extension products with the predicted sizes for the two major transcripts A and B (328 and 201 bases, respectively).

stabilized at a slightly lower level (Fig. 6). Similar S1 nuclease analyses of globe RNA (retina as well as iris) showed a roughly twofold increase after birth, with a peak at 14 to 17 days, somewhat earlier than in the cortex (data not shown). Heart RNA also showed a doubling in NGF expression by 17 days, which was followed by a considerable decline (data not shown). At all times transcript B predominated over A (four- to eightfold as determined by densitometry) in the different tissues. The patterns remained stable from 4 weeks to adulthood (Fig. 7).

Using a probe with a high specific activity for transcript C, we detected a faint signal with the submaxillary gland, the 10-week heart and adult cortex total RNA (Fig. 8). Unlike the salivary gland where the level of C relative to that of B and A was very low (less than 1% of the total NGF RNA), the level of transcript C in cortex and heart made up 5 to 10% of total NGF mRNA.

Effect of whisker removal and consequent rearrangement of sensory pathway on NGF transcript levels. Synaptogenesis occurs at roughly the same time in development as the observed changes in the level of NGF transcripts. To determine whether synaptogenesis has a role in causing the initial rise and later stabilization of NGF mRNA in the cortex, we attempted to prevent the normal formation of synapses in that brain region. For these experiments, we have used the mouse whisker pad system with its convenient internal control (the opposite side) (34). This system has revealed the importance of sensory experience in the formation of certain neural networks. Three neurons connect whiskers to the rodent somatosensory cortex. Removal of the right whisker at birth disrupts the development of these neurons. Axons from the second neuron in the pathway (with its cell body in the left thalamus) then fail to reach their target cells (in the left cortex) as they would normally (34). While it is not known whether the thalamocortical connection involves NGF, sensory deprivation at this stage of development dramatically disturbs the architecture of the somatosensory cortex. We removed the right whisker pads of mice within 1 day after birth. (Subsequent examination at 4 weeks after birth showed no regrowth of whiskers.) S1 nuclease protection analysis showed no difference in NGF mRNA expression (Fig. 7), at 4 weeks in the relevant somatosensory cortex. The extra band present only on the left and seen in various other S1 nuclease assays, appears to be specific but is of unclear origin. Attempts to clone other cDNAs that might correspond to this species have failed. Because we may have missed the critical time in which a lesion could produce an effect, we also removed whisker pads at 1, 2, and 3 weeks after birth; somatosensory deprivation beginning at these times also had no effect on the levels of cortical NGF transcripts at 4 weeks after birth (data not shown). Additionally, the lesions produced no alteration in 4-week NGF

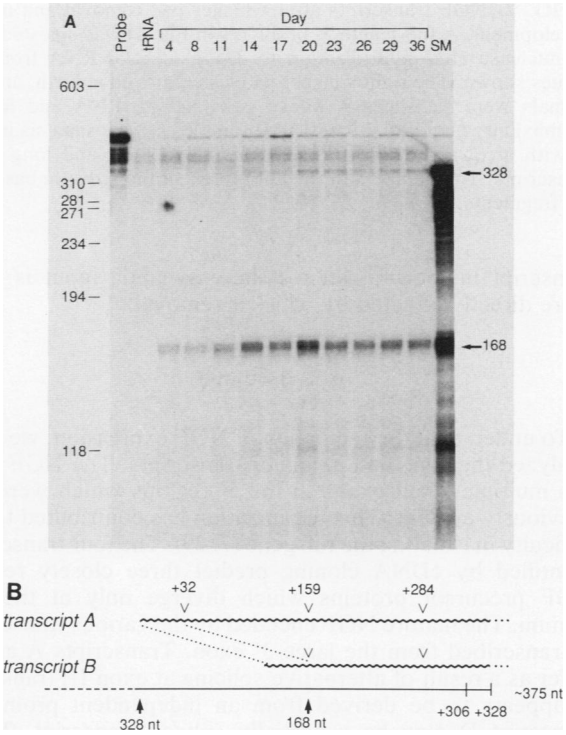

FIG. 6. (A) S1 nuclease analysis of NGF transcripts from the developing mouse cortex. A 25-μg portion of total RNA from mouse cortex from the postnatal period shown was hybridized to a probe representing the full 5′ end of NGF transcript A. Probe fragments protected from S1 nuclease digestion by the RNA were separated on a 5% urea–acrylamide gel; the dried gel was exposed with an intensifying screen at −70°C for 1 week. SM denotes female submaxillary gland total RNA (less than 5 μg), and yeast tRNA was used as a negative control. Arrows indicate the sizes predicted for fragments protected by transcripts A and B. The numbers to the left represent the sizes (in bases) of fragments from a *Hae*III digest of φX174 DNA. (B) Diagram of the two major NGF transcripts (wavy lines) in relation to the S1 nuclease probe (straight line). Transcripts A and B differ only in the presence of the second exon (+32 to +159 of A). The probe was synthesized on a single-stranded M13 template (subcloned from a full-length cDNA A) with a primer complementary to +328 to +306. Arrows indicate the sites of cleavage in the probe depending on whether it is protected by transcript A (328 nucleotides [nt]) or B (168 nt).

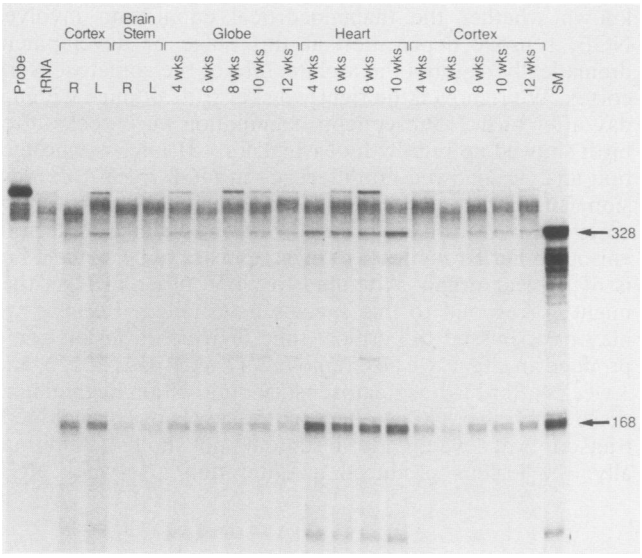

FIG. 7. NGF transcripts after whisker pad removal and in late development. A full-length 5′ probe (as in Fig. 5) was digested with S1 nuclease after hybridization to 25 μg of total RNA from the tissues shown. The right whisker pad was removed at birth, and the animals were sacrificed 4 weeks (wks) later; tRNA and female submaxillary gland total RNA (SM) samples are the same as in Fig. 5, with arrows showing the sizes of major short and long NGF transcripts. The numbers to the left represent the sizes (in bases) of the fragments. R, Right; L, left.

transcript in the brainstem (where synaptic input is even more directly affected by whisker removal).

DISCUSSION

To understand the regulation of NGF expression, we have analyzed the gene and its major transcripts. The NGF gene has multiple small exons in the 5′ regions which were not previously evident. This organization has contributed to the difficulty in isolating the full gene (7, 29). The four transcripts identified by cDNA cloning predict three closely related NGF precursor proteins which diverge only at their N termini. The mature NGF encoded by the various transcripts is transcribed from the large 3′ exon. Transcripts A and B differ as a result of alternative splicing at exon II; transcript C appears to be derived from an independent promoter; transcript D may be a partially spliced transcript. Thus, NGF gene expression is probably regulated by transcription initiation and by RNA processing.

Significantly, the sequence differences in the N termini of the precursors alter the position of the hydrophobic domain assumed to function as a signal peptide; whereas the precursor predicted by transcripts B and D has this domain in the N-terminal position, transcripts A and C predict proteins with the same hydrophobic sequence about 70 amino acids from the N terminus. The differences in structure might signify functional differences of these precursors. These putative functional differences could be reflected in distinctive transcriptional patterns in different tissues and throughout development. However, we have found that all tissues, except for mouse submaxillary gland and the placenta (Edwards et al. [8]), have the same profile of transcripts. Transcript B predominates, with A present at 20 to 30% of this level and C and D at barely detectable levels. In mouse submaxillary gland (and placenta), transcript A is the major form, with B at 30% and C and D at 0.1 to 1.0% the level of A. During postnatal development, A and B change in parallel. Transcript C appears at a higher level relative to A and B in cortex and heart, compared with the salivary gland. Thus its promoter can be independently regulated. This observation, however, does not necessarily imply a separate function for the C-encoded prohormone, especially in light of the very low abundance of this transcript.

These data do not allow us to conclude whether the precursors predicted by transcripts A and B have unique functions. The constant ratio of A to B may reflect a property common to innervated tissues that is not shared by the mouse submaxillary gland and the placenta. On the other hand, the data are compatible with the notion that A and B are functionally equivalent. In fact, in expression experiments, both precursors give rise to mature NGF with similar facility (R. H. Edwards, M. Selby, and W. J. Rutter, unpublished data).

The quantity of total NGF mRNA changes during the postnatal period. Whittemore et al. (32) have shown an increase in NGF mRNA in brain that plateaus 3 to 4 weeks after birth. Large et al. (16) have verified the rise in cortical NGF message with a decline after the peak at 3 weeks. We have confirmed the increase, decrease, and then stabilization of NGF mRNA levels with respect to total RNA, but the magnitude of change (two- to fourfold) is less than that seen by Large et al. (ca. eightfold). The difference may be attributable to the marked neonatal variation in the proportion of total brain RNA that is mRNA. The significance of these changes is unclear; they may only reflect a variable dilution of NGF transcripts by the rapidly changing RNA content of these tissues.

The changes in NGF gene expression coincide with synapse formation in the tissues examined. In the central and peripheral nervous systems, exemplified by the cortex and heart, the majority of ingrowing nerve terminals arrive at their target organ before birth. One large afferent pathway to

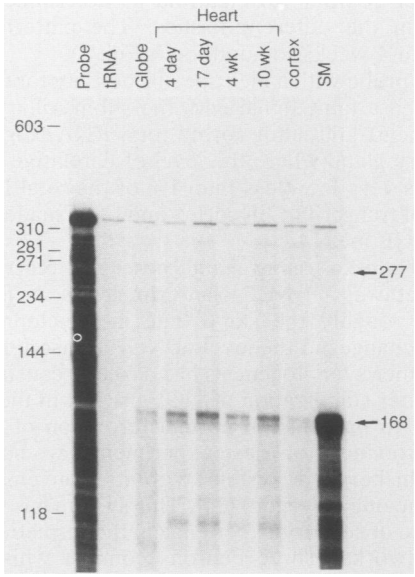

FIG. 8. S1 nuclease analysis of transcripts corresponding to NGF cDNA C. The probe used is described in the legend to Fig. 2. Standards (left) are a *Hae*III digest of ϕX174 DNA. Arrows at the right denote the predicted sizes for the protected fragments. wk, week; SM, female submaxillary gland total RNA.

the cortex originates in the thalamus. Its axons reach the cortex at birth and approach the cells destined for innervation shortly thereafter. However, the connections between thalamic and cortical cells continue to mature physiologically for weeks (13, 33). Postganglionic sympathetic neuronal processes are present in the heart before birth (7) but do not develop varicosities until later; the connection does not become fully functional until 2 weeks after birth (31).

Because the period during which NGF exerts its critical effect on neuronal survival overlaps the maturation of synaptic contacts, we attempted to ask whether innervation per se causes the developmental changes in NGF expression. Since NGF transcripts increase and then stabilize, in the developing cortex, whisker pad removal might alter this pattern of NGF expression. We analyzed whisker pad RNA at 4 weeks, just after the peak of NGF expression and presumably a sensitive time in development. We were unable to observe any change in the expression of the two principal NGF transcripts, A and B (Fig. 6). Because the critical window of responsiveness to sensory deprivation might occur later, we performed the same lesion at 1, 2, and 3 weeks after birth; there was no detectable change in NGF gene transcripts at 4 weeks. The failure to observe changes in NGF transcripts during this critical developmental period suggests that innervation does not regulate NGF mRNA expression. Explantation of the adult rat iris does result in a 10- to 20-fold increase in NGF transcripts, but sympathetic and sensory denervation of the iris in situ does not produce any increase in NGF mRNA (26). In both systems, innervation does not control NGF RNA expression. These experiments do not eliminate the possibility that NGF transcripts in supporting cells (e.g., fibroblasts and Schwann cells) change during regeneration or after injury. However, there is no evidence from these experiments of a sensitive system of feedback regulation operating at the level of NGF transcripts. We hypothesize that the apparent invariant nature of this expression is a reflection of the inherent capacity of the target cells to be innervated.

The low level of NGF expression and the lack of feedback control is compatible with a hypothesis accounting for selective cell death in the development of NGF-responsive neuronal networks. We presume that the two cell types making NGF, neural supporting cells (e.g., Schwann cells) and innervated cells, both synthesize NGF at low levels, but the innervated cells are the major supply at least during development. We assume that NGF acts only in close proximity to the producing cells. In the region of the synapse, a special circumstance may exist; NGF secreted by the incipient innervated cell may in part determine the extent of innervation. Indeed, NGF secretion could even be localized to the site of incipient synapse formation. The NGF receptors of developing nerve fibers may then bind the NGF and remove significant quantities via the axonal transport system. Innervating cells in the vicinity then compete for the limiting available NGF according to (i) proximity to the NGF source, (ii) the number and affinity of NGF receptors on the nerve terminal, and (iii) some aspect of neural activity (e.g., recycling of nerve terminal membrane). The axon in the most favorable anatomical and function position eventually becomes the dominant consumer of the local supply of NGF while the availability to others is reduced. Supply to the neurons competing successfully could occur via some specialized aspect of the synapse structure. In this fashion the neurons with the appropriate connections live, while the others receive an inadequate supply of NGF, and die.

ACKNOWLEDGMENTS

We thank Leslie Spector for preparing the manuscript, Philip Barr and Jennifer Barnett for preparing oligonucleotides, and James Ou for helpful discussions.

R.E. is the recipient of a postdoctoral fellowship from the National Institute of Neurological and Communicative Disorders and Stroke (NS07529). This research was funded by Public Health Service grant AM 21344 from the National Institutes of Health to W.J.R.

LITERATURE CITED

1. **Angeletti, P. U., R. Levi-Montalcini, and F. Caramia.** 1971. Ultrastructural changes in sympathetic neurons of newborn and adult mice treated with Nerve Growth Factor. J. Ultrastruct. Res. **36**:24–36.
2. **Benoist, C., K. O'Hare, R. Breathnach, and P. Chambon.** 1980. The ovalbumin gene-sequence of putative control regions. Nucleic Acids Res. **8**:127–142.
3. **Cathala, G., J. F. Savouret, B. Mendez, B. L. West, M. Karin, J. Martial, and J. D. Baxter.** 1983. A method for isolation of intact, translationally active RNA. DNA **2**:329–335.
4. **Chirgwin, J. M., A. E. Przybyla, R. J. MacDonald, and W. J. Rutter.** 1979. Isolation of biologically active ribonucleic acid from sources enriched in ribonuclease. Biochemistry **18**:5294–5299.
5. **Corden, J., B. Wasylyk, A. Buchwalder, P. Sassone-Corsi, C. Kedinger, and P. Chambon.** 1980. Promoter sequences of eucaryotic protein-coding genes. Science **209**:1406–1414.
6. **Darby, J. K., J. Feder, M. Selby, V. Riccardi, R. Ferrell, D. Siao, K. Goslin, W. J. Rutter, E. M. Shooter, and L. L. Cavalli-Sforza.** 1985. A discordant sibship analysis between beta Nerve Growth Factor and neurofibromatosis. Am. J. Hum. Genet. **37**:52–59.
7. **Champlain, J., T. Malmfors, L. Olson, and C. Sachs.** 1970. Ontogenesis of peripheral adrenergic neurons in the rat: Pre- and postnatal observations. Acta Physiol. Scand. **80**:276–288.
8. **Edwards, R. E., M. Selby, and W. J. Rutter.** 1986. Differential RNA splicing predicts two distinct Nerve Growth Factor precursors. Nature (London) **319**:784–787.
9. **Gorin, P. D., and E. M. Johnson.** 1979. Experimental autoimmune model of nerve growth factor deprivation: effects on developing peripheral sympathetic and sensory nerves. Proc. Natl. Acad. Sci. USA **76**:5382–5386.
10. **Gubler, U., and B. J. Hoffman.** 1983. A simple and very efficient method for generating cDNA libraries. Gene **25**:263–269.
11. **Hendry, I. A.** 1975. The response of adrenergic neurons to axotomy and nerve growth factor. Brain Res. **94**:87–97.
12. **Herrup, K., and H. Thoenen.** 1979. Properties of the nerve growth factor receptor of a clonal line of rat pheochromacytoma (PC-12) cells. Exp. Cell Res. **121**:71–78.
13. **Hubel, D., T. N. Weisel, and S. LeVay.** 1977. Plasticity of ocular dominance columns in the monkey striate cortex. Philos. Trans. R. Soc. Lond. B. Biol. Sci. **278**:377–409.
14. **Johnson, E. M., R. Y. Andres, and R. A. Bradshaw.** 1978. Characterization of the retrograde transport of nerve growth factor (NGF) using high specific activity ^{125}I-NGF. Brain Res. **150**:319–331.
15. **Korshing, S., and H. Thoenen.** 1983. Nerve growth factor in sympathetic ganglia and corresponding target organs of the rat: correlation with the density of sympathetic innervation. Proc. Natl. Acad. Sci. **80**:3513–3516.
16. **Large, T., S. Bodary, D. Clegg, G. Weskamp, U. Otten, and L. Reichardt.** 1986. Nerve growth factor gene expression in the developing rat brain. Science **234**:352–355.
17. **Levi-Montalcini, R.** 1966. The nerve growth factor: its mode of action on sensory and sympathetic nerve cells. Harvey Lect. **60**:217–259.
18. **Levi-Montalcini, R., and B. Booker.** 1960. Destruction of the sympathetic ganglia in mammals by an antiserum to the nerve growth factor protein. Proc. Natl. Acad. Sci. USA **46**:384–390.
19. **Maniatis, T., E. F. Fritsch, and J. Sambrook.** 1982. Molecular cloning, a laboratory manual. Cold Spring Harbor Laboratory,

Cold Spring Harbor, N.Y.
20. **Maxam, A., and W. Gilbert.** 1980. Sequencing end-labeled DNA with base specific chemical cleavages. Methods Enzymol. **65**:499–560.
21. **Mount, S. M.** 1982. A catalogue of splice junctions sequences. Nucleic Acids Res. **10**:459–472.
22. **Reynolds, G. A., J. L. Goldstein, and M. S. Brown.** 1985. Multiple mRNAs for 3-hydroxy-3-methylglutaryl coenzyme A reductase determined by multiple transcription initiation sites and intron splicing sites in the 5′ untranslated region. J. Biol. Chem. **260**:10369–10377.
23. **Sanger, F., S. Nicklen, and A. R. Coulson.** 1977. DNA sequencing with chain terminating inhibitors. Proc. Natl. Acad. Sci. USA **74**:5463–5467.
24. **Scott, J., M. Selby, M. Urdea, M. Quiroga, G. I. Bell, and W. J. Rutter.** 1983. Isolation and nucleotide sequence of a cDNA encoding the precursor of mouse nerve growth factor. Nature (London) **302**:538–540.
25. **Shelton, D. L., and L. F. Reichardt.** 1984. Expression of the beta nerve growth factor gene correlates with the density of sympathetic innervation in effector organs. Proc. Natl. Acad. Sci. USA **81**:7951–7955.
26. **Shelton, D. L., and L. F. Reichardt.** 1986. Studies on the regulation of beta nerve growth factor gene expression in iris: the level of mRNA encoding nerve growth factor is increased in iris in explant cultures in vitro, but not in irises deprived of sensory or sympathetic innervation in vivo. Proc. Natl. Acad. Sci. USA **83**:2714–2718.
27. **Stockel, K., M. E. Schwab, and H. Thoenen.** 1975. Comparison between the retrograde axonal transport of nerve growth factor and tetanus toxin in motor, sensory and adrenergic neurons. Brain Res. **99**:1–16.
28. **Thoenen, H., and Y. A. Barde.** 1980. Physiology of nerve growth factor. Physiol. Rev. **60**:1284–1335.
29. **Ullrich, A., A. Gray, C. Berman, and T. J. Dull.** 1983. Human beta nerve growth factor gene sequence highly homologous to that of mouse. Nature (London) **303**:821–825.
30. **Valerio, D., M. G. C. Doyvesteyn, B. M. M. Dekker, L. Van Des Voorn, H. van Ormondt, and A. J. Van der Eb.** 1985. Adenosine deaminase characterization and expression of a gene with a remarkable promoter. EMBO J. **4**:437–443.
31. **Wekstein, D. R.** 1965. Heart rate of the preweaning rat and its autonomic control. Am. J. Physiol. **208**:1259–1262.
32. **Whittemore, S. R., T. Ebendal, L. Larkfors, L. Olson, A. Seiger, I. Stromberg, and H. Persson.** 1986. Developmental and regional expression of beta NGF mRNA and protein in the rat central nervous system. Proc. Natl. Acad. Sci. USA **83**:817–821.
33. **Wise, S. P., and E. G. Jones.** 1978. Developmental studies of thalamocortical and commissural connections in the rat somatic sensory cortex. J. Comp. Neurol. **178**:187–208.
34. **Woolsey, T. A., D. Durham, R. M. Harris, D. J. Simons, and K. C. Valentine.** 1981. Somatosensory development, p. 259–292. *In* Development of perception, Vol. I, Academic Press, Inc., New York.